Title
Nonuniform allocation of hippocampal neurons to place fields across all hippocampal subfields

Journal
Hippocampus, 26(10)

ISSN
1050-9631

Authors
Witharana, WKL
Cardiff, J
Chawla, MK
et al.

Publication Date
2016-10-01

DOI
10.1002/hipo.22609

Peer reviewed

HHS Public Access

Author manuscript

Hippocampus. Author manuscript; available in PMC 2022 January 19.

Published in final edited form as:

Hippocampus. 2016 October ; 26(10): 1328–1344. doi:10.1002/hipo.22609.

Nonuniform Allocation of Hippocampal Neurons to Place Fields Across All Hippocampal Subfields

W.K.L. Witharana[1], **J. Cardiff**[1], **M.K. Chawla**[2], **J.Y. Xie**[1], **C.B. Alme**[1,3], **M. Eckert**[1], **V. Lapointe**[1], **A. Demchuk**[1], **A.P. Maurer**[4], **V. Trivedi**[1], **R.J. Sutherland**[1], **J.F. Guzowski**[5], **C.A. Barnes**[2], **B.L. McNaughton**[1,5,*]

[1]Canadian Centre for Behavioural Neuroscience, University of Lethbridge, T1K 3M4

[2]Evelyn F. McKnight Brain Institute, University of Arizona, Tucson, Arizona

[3]Kavli Institute for System Neuroscience and Centre for Neural Computation, Norwegian University of Science and Technology, Trondheim, Norway

[4]Department of Neuroscience, College of Medicine, University of Florida, Gainesville, Florida

[5]Center for Neurobiology of Learning and Memory, Department of Neurobiology and Behavior, University of California, Irvine

Abstract

The mechanisms governing how the hippocampus selects neurons to exhibit place fields are not well understood. A default assumption in some previous studies was the uniform random draw with replacement (URDWR) model, which, theoretically, maximizes spatial “pattern separation”, and predicts a Poisson distribution of the numbers of place fields expressed by a given cell per unit area. The actual distribution of mean firing rates exhibited by a population of hippocampal neurons, however, is approximately exponential or log-normal in a given environment and these rates are somewhat correlated across multiple places, at least under some conditions. The advantage of neural activity-dependent immediate-early gene (IEG) analysis, as a proxy for electrophysiological recording, is the ability to obtain much larger samples of cells, even those whose activity is so sparse that they are overlooked in recording studies. Thus, a more accurate representation of the activation statistics can potentially be achieved. Some previous IEG studies that examined behavior-driven IEG expression in CA1 appear to support URDWR. There was, however, in some of the same studies, an under-recruitment of dentate gyrus granule cells, indicating a highly skewed excitability distribution, which is inconsistent with URDWR. Although it was suggested that this skewness might be related to increased excitability of recently generated granule cells, we show here that CA1, CA3, and subiculum also exhibit cumulative under-recruitment of neurons. Thus, a highly skewed excitability distribution is a general principle common to all major hippocampal subfields. Finally, a more detailed analysis of the frequency distributions of IEG intranuclear transcription foci suggests that a large fraction of hippocampal neurons is virtually silent, even during sleep. Whether the skewing of the excitability distribution

*Correspondence to: Dr. Bruce McNaughton, Canadian Centre for Behavioural Neuroscience, The University of Lethbridge, 4401 University Drive West, Lethbridge, AB, T1K 3M4, Canada. bruce.mcnaughton@uleth.ca.

is cell-intrinsic or a network phenomenon, and the degree to which this excitability is fixed or possibly time-varying are open questions for future studies.

Keywords

place cells; remapping; immediate early genes; hippocampus; place allocation

INTRODUCTION

Efficient spatial learning is critically dependent on the hippocampal formation (O'Keefe and Nadel, 1978), and hippocampal principal neurons exhibit discrete patches of high firing rates called "place fields", which, for a given cell, appear randomly dispersed. Together, they provide a sparse, distributed, ensemble code or "cognitive map" for spatial location (O'Keefe and Dostrovsky, 1971; Thompson and Best, 1989). The ratio of "active" to "non-active" neurons over a region of space of given area increases systematically across hippocampal subfields dentate gyrus, CA3, CA1 and subiculum (Barnes et al., 1990), and decreases systematically along the septotemporal axis of the hippocampus, in conjunction with an increase in place field size (Jung et al., 1994; Maurer et al., 2005; Kjelstrup et al., 2008). Most, but not all, place fields appear during the animal's first entry into the location (Hill, 1978; Wilson and McNaughton, 1993) and the location of the field can remain stable over many days under some conditions (Thompson and Best, 1990; Mankin et al., 2012; Ziv et al., 2013); however, place fields can be added or removed from the "map" (Frank et al., 2004; Lee et al., 2012; Monaco et al., 2014; Mankin et al., 2015) and within-field firing rates can also modulate up or down (Leutgeb et al., 2005; Navratilova et al., 2012), at least partly as a function of experience. While these characteristics may reflect components of episodic memory, the actual mechanisms governing the allocation of cells to place fields are not well understood.

The hippocampus has been suggested to perform "pattern separation", such that small differences in input (particularly location) produce larger differences in firing patterns, thus reducing interference in associative memory (Marr, 1971; McNaughton and Nadel, 1990; Treves and Rolls, 1992; O'Reilly and McClelland, 1994). Pattern separation is a natural consequence of the apparently random allocation of place fields (Rich et al., 2014). Such "global remapping" (Bostock et al., 1991; Leutgeb et al., 2005; Leutgeb et al., 2007; Alme et al., 2014) implies that the population firing rate vectors for different, widely separated places are statistically uncorrelated. To be maximally uncorrelated, however, would mean that cells would have to be allocated to express place fields by a process equivalent to uniform random draw with replacement (URDWR). In such a model, each cell has an equal probability of being allocated at random to fire in a given location.

Consistent with the random draw assumption, a given place cell can have multiple place fields in an environment (Park et al., 2011), and, in contrast, for example, to medial entorhinal grid cells (Hafting et al., 2005), the distance between place fields is unpredictable. Indeed, if place fields are defined on the basis of a cycle of phase precession, then field centers can sometimes be so close together that the fields overlap, resulting in doublets of

spike phases (Maurer et al., 2006). In other cases, two fields from the same cell can be as far apart as possible in an environment of fixed size, or there may be only one or no fields. But is the probability of allocation of a field in a given small space uniform across the population of cells? URDWR predicts a Poisson distribution for the number of place fields exhibited by each cell in a given environment, but at least four studies show that the distribution is very "heavy tailed" (Shen et al., 1997; Maurer et al., 2006; Burke et al., 2011; Rich et al., 2014). The mean firing rate distributions of hippocampal principal cells is also highly skewed and varies systematically across hippocampal subfields (Barnes et al., 1990), more closely approximating a log-normal rather than a normal distribution, and firing rates can be somewhat correlated across different sleep-wake states and across behaviors in different environments (Mizuseki and Buzsáki, 2013). These findings alone do not necessarily contradict URDWR, because, the selection of which neurons are active in a location could be to some extent independent of in-field firing rates, but the firing rate data are consistent with the measured place field distributions, and Rich *et al.* (2014) showed that, in CA1 at least, there is no relationship between number of fields expressed on a large track and in-field firing rate. Moreover, the discovery of "pre-play" of hippocampal temporal sequences in pre-experience sleep (Dragoi and Tonegawa, 2011; Dragoi and Tonegawa, 2013) suggests that some neurons may be "pre-selected" for activation. Such pre-selection could be due to nonuniform intrinsic excitability (Epsztein et al., 2011) or a preconfiguration of the hippocampal network (McNaughton et al., 1996; Samsonovich and McNaughton, 1997) that may emerge during development (Deguchi et al., 2011; Xu et al., 2014), or a combination of these effects. Thus, although the distribution of place fields of a given cell in a large space appears to be random, the propensity to form fields (i.e., the total number that would be seen in a large space) is apparently highly skewed in the population, more consistent with a Non-uniform Random Draw With Replacement model (NRDWR). Whether this propensity is fixed or possibly variable over time, however, is unknown.

One limitation of electrophysiological recordings is the relatively small yield of detected units and the failure to count neurons that fire very few or no spikes during the recording session. Indeed, as Henze and colleagues (Henze et al., 2000) have pointed out, the number of neurons that should be "seen" by a tetrode in CA1 is substantially larger than the number of clusters that are actually extracted from a recording session, suggesting that most cells are extremely silent most of the time, emitting either no spikes or too few to form isolatable clusters. While some may argue that Henze *et al.* overestimate the number of cells that should be detected, they are unlikely to have overestimated this value by more than a factor of five, in which case, there would still be an underestimate of 2×, even if it were true that a tetrode in CA1 records on average 10 isolatable cells. In our experience, this is an overestimate and the actual number is closer to 5. As such, even a conservative estimation of the "unseen" population in recordings would leave a considerable number of neurons undetected in a typical electro-physiological experiment. In addition, obtaining large single unit samples from multiple brain regions in the same rats, or even different rats in different experiments, is time and labor intensive and technically very challenging.

Immediate-early gene (IEG) activation measures on the other hand, while of limited temporal resolution, provide the opportunity, under certain conditions, to assess the distribution of activity in much larger populations, including extremely silent cells. The

patterned activity elicited by hippocampal principal cells during spatial exploration triggers simultaneous transcription of IEGs such as *Homer1a (H1a)* and *Arc*, two co-regulated genes that are critical for memory consolidation and synaptic plasticity (Guzowski et al., 2000). The induction of IEG transcription leads to the reliable appearance of punctate nuclear transcription foci of *Arc* mRNA (beginning ~2 min and peaking about 5–8 min post-activation) and *Homer1a* mRNA (25–30 min post activation) in activated hippocampal neurons. As such, these two genes are commonly used as visual markers of cellular activity which occurred within a certain window of time prior to sacrifice. One caveat, however, is that the dependence of expression on spiking activity *per se* may be both brain-state and experience dependent and, for example is severely diminished in hippocampus by reversible medial septal inactivation with tetracaine (Miyashita et al., 2009). Data derived from some IEG activation studies report largely uncorrelated hippocampal activation patterns across different environments (Guzowski et al., 1999; Vazdarjanova and Guzowski, 2004; Burke et al., 2005; Rosi et al., 2009; Marrone et al., 2014). For example, using the neural activity marker *Arc*, Guzowski *et al.* (1999) observed that about 40% of CA1 pyramidal neurons were activated in one environment, whereas the overlap for two environments of the same size was close to the 16% as would be predicted by URDWR. Not all studies, however, report such a high degree of statistical independence for hippocampal IEG activation in two spatial contexts, suggesting that the excitability distribution may sometimes be highly skewed: the CA1 activity in Vazdarjanova and Guzowski (2004) had a higher similiarity score than 0—i.e., it was not statistically uncorrelated; Chawla *et al.* (2005) reported that the proportion of granule cells exhibiting exploration-induced *Arc* activation in *only* the second of two sequentially visited environments (nuclear-only signal) was much less than predicted by URDWR (0.006 instead of ~0.02); finally Alme *et al.* (2010) found substantial under-recruitment of granule cells during successive visits to four familiar environments as compared to repeated visits to the same environment. Alme *et al.* speculated that this under-recruitment may be related to enhanced excitability of recently generated granule cells (the “early retirement” hypothesis); however, as we report here, the same pattern has now been found from the same tissue (see below) in CA1 and CA3, which do not exhibit postnatal neurogenesis.

Here, we present data from seven IEG studies, including an analysis of CA3 and CA1 from the same tissue from which Alme *et al.* (2010) analyzed the dentate gyrus, and including results from the dorsal subiculum in some experiments. Four of these studies quantified *Homer1a* intranuclear foci to measure activated hippocampal cells during extended or massed spatial exploration epochs because the *Homer1a* primary transcript is ~55 kb in length (Bottai et al., 2002) which causes the transcription foci to appear in nuclei of activated cells at ~25–40 min when using a riboprobe targeting the 3′ UTR and to persist longer than *Arc* transcripts. One study measured *Arc* expression; and two other studies used both *Arc* and *Homer1a* for dual-epoch catFISH analysis (cellular compartment analysis of temporal activity by fluorescence *in situ* hybridization (Guzowski et al., 2005)). In addition, we reanalyzed neural ensemble recording data from Maurer *et al.* (2006) which computed place field distributions on large and small circular tracks, a behavioral paradigm that closely resembles one of the IEG studies described here. We also found activation proportions in another published unit recording study, Alme *et al.* (2014), which adopted a similar

multi-environmental paradigm as our multiple-place IEG experiments, and we included their published ratios for comparison. Taken together, these data converge on the conclusion that the probability of allocation of place fields per unit of space is highly nonuniform in all hippocampal subfields, in spite of wide variations in the total recruitment per unit space across subfields.

METHODS

Uniform Random Draw with Replacement (URDWR) Model Assumptions

URDWR implies that all cells have the same probability of activation in an environment of a given size (P_1), and consequently the probability that a cell is activated in both of two arbitrary environments is P_1^2. In general, given P_1 then the expected cumulative total activation of cells for x environments of the same size (or for a single environment "x" times the size of environment 1) is:

$$P_X = \left(1 - (1 - P_1)^X\right)$$

This relationship can be used in two ways. First, given the ratio of numbers of activated cells in x and 1 environments of equal size (P_x/P_1) one can estimate P_1 (under URDWR) without actually measuring the ratio of active to inactive cells, since the denominators cancel out. Alme *et al.* (2010) found in DG that this estimate was far above P_1 measured from actual cell counts, indicating a highly skewed activation probability inconsistent with URDWR. Alternatively, given an estimate of P_1 for an environment of unit size, the relationship can be used to calculate (under the URDWR assumption) the expected activation ratio for multiple environments of total area x. The latter method provides a simple graphical visualization of the extent to which the cumulative activation of cells as total explored space increases underestimates the URDWR prediction (Fig. 1).

Immediate-Early Gene Studies

Behavioral procedures—On the basis of different behavioral paradigms, the seven IEG studies included in this meta-analysis can be divided into three main groups:

1. Multiple Place (MP) experiments (studies MP1, MP2, MP3, MP4): Four studies used multiple place designs in which rats were successively exposed to different environments without breaks, and IEG activation was compared to rats exposed to a single environment.
2. Circle Track (CT) experiment (CT5): In one study, rats were trained to run on two circular tracks. One track was four times the area of the smaller track.
3. AB/AA experiments (studies AB6 and AB7): Two dual-IEG studies exposed rats to two 5 min environmental epochs, either the same room twice, or two different rooms. Exposures were separated by 20 min.

Studies MP1, MP2, MP3, CT5, AB6, and AB7 were conducted at the University of Lethbridge (Lethbridge, Alberta, Canada). All animal handling adhered to regulations according to the Canadian Council on Animal Care. Experimental procedures were approved

by the University of Lethbridge Animal Welfare Committee. Study MP4 was conducted at the University of Arizona (Tucson, Arizona, USA), and detailed methods were published previously (Alme et al., 2010).

MP1, MP2, and MP3: Rats were housed in colony room home-cages and transport cages which were clear plastic shoebox size containers which measured 24 cm × 45.5 cm × 21 cm. Prior to each experimental test day, rats were handled for 5–10 min per day for at least 2 weeks (unless otherwise indicated). Positive controls were MECS (maximal electroconvulsive shock) subjects that received a brief electrical stimulus via ear clips connected to a research-grade ECT machine (Ugo Basile, Italy) with parameters prescribed by the manufacturer (frequency of 100 pulses/s; pulse width of 0.5 ms, 1.1 s pulse-train duration, and 85 mA current). All three studies employed *Homer1a* intranuclear transcription foci analysis to quantify activation in hippocampal populations.

MP1: Data consist of subjects in the covered-transport group reported in Witharana, 2011 (MSc Thesis, University of Lethbridge, Witharana, 2011). Naïve, male Long-Evans rats (n = 21) aged 3–7 months were divided in two test groups: one-environment exposure (1E, n = 6), or five-environment (5E, n = 7) exposure; and two control groups: home-cage (HC, n = 4) or maximal electroconvulsive shock positive control (MECS, n = 4). All subjects were acclimated to a small, dark antechamber for 3–4 hours per day for two weeks prior to the test day. This maintenance in the dark room was in effort to ensure the cage control condition was one in which the animals had minimal disturbance from noise of other animals, or animal care staff. On test day, rats rested in the darkened antechamber in home-cages for a minimum of one hour to ensure quiescence and minimal IEG expression. Transport of 1E and 5E animals between the holding room and test environments occurred with the transport cages covered with a dark blanket. Rats in the 1E condition were introduced to a triangular enclosure in a novel test room, allowed to explore freely for 5 min, and returned to the darkened antechamber to rest for 25 min before sacrifice. Rats in the 5E condition were exposed to 5 consecutive environments with each exposure lasting 2 min, and then returned to the darkened antechamber to rest for 25 min before sacrifice. The order of environments exposed were: a triangular enclosure (also navigated by 1E rats) (area = 3402 cm^2), a square enclosure on a wooden desk (5041 cm^2), a trapezoid metal tank (6480 cm^2), a circular track elevated by 19cm (4449 cm^2), and another square enclosure with 3 pillars scattered within (5041 cm^2). During all unrestrained exploration, the experimenter ensured that the rat traversed all parts of the enclosure as indicated by grid markings on the floor of each enclosure. In total, the 5E rats were exposed to 24,413 cm^2 of area when all novel environments were combined; while 1E rats were exposed to 3402 cm^2. This gives a ratio of approximately x = 7 (7.18) when we consider the increased area of space experienced (x in the URDWR model) by the 5E versus 1E groups (Table 1). Home-cage (HC) controls were never transported out of this dark antechamber to the experiment rooms, but instead were directly removed from the darkened antechamber and then sacrificed after a quiescent period of 2–3 hours. MECS positive controls received ECT shock, rested for 25 min, and were then sacrificed by decapitation. *Homer1a* activation analysis was performed to quantify activation proportions in CA3, CA1, and dorsal subiculum.

MP2: These data consist of subjects in the uncovered-transport group reported in Witharana, 2011 (MSc Thesis, University of Lethbridge, Witharana, 2011). Naïve, male Long-Evans ($n = 22$) and Brown Norway ($n = 6$) rats aged 3–7 months were divided into two test groups: one-environment exposure (1E, $n = 8$), or five-environment (5E, $n = 8$) exposure; and two control groups: home-cage (HC, $n = 6$) or maximal electroconvulsive shock positive control (MECS, $n = 6$). All subjects were acclimated to a small, dark antechamber for 3–4 hours per day for two weeks prior to test day. This maintenance in the dark room was in effort to ensure the cage control condition was one in which the animals had minimal disturbance from noise of other animals, or animal care staff. Once per day for three days prior to testing, rats were transported to all test rooms but remained in their cages in each room, as transport habituation. This additional transport habituation period is different from procedures in MP1 which lacked this habituation period. On the test day, all rats rested in an undisturbed, darkened antechamber in their home-cages for a minimum of one hour to ensure quiescence and minimal IEG expression. Rats in the 1E and 5E conditions were treated identically to the MP1 group, except that their transport to the environments was in an uncovered transport cage rather than a covered one. Home-cage (HC) controls were never transported out of the dark antechamber to the experiment rooms, but instead were directly removed from the darkened antechamber and then sacrificed after a quiescent period of 2–3 hours. MECS positive controls received ECT shock, rested for 25 min, and were then sacrificed by decapitation. The 5E rats were exposed to a total of 24, 413 cm^2 of area when all novel environments were combined; while 1E rats were exposed to 3402 cm^2. This gives a ratio of approximately $x = 7$ (7.18) when we consider the increased area of space experienced (x in the URDWR model) by the 5E versus 1E groups (Table 1).

MP3: Data included here are derived from sham controls reported in Cardiff, 2012 (MSc Thesis, University of Lethbridge, Cardiff, 2012). Naïve, male Long-Evans rats ($n = 10$), 5 months old, underwent sham surgeries while experimental counterparts (excluded from this data) received adrenalectomies. These control rats received pre-surgical anaesthetic infusions, and received only subcutaneous incisions in the flank, a relatively non-invasive surgery. Rats recovered from the sham surgeries for 12 weeks. On test day, rats were exposed to either the same novel environment 5 times in a row (AAAAA), or 5 novel environments in succession (ABCDE). These environments were located in different rooms and rats were transported in a clear, uncovered transport cage, lined with corncob bedding. Each of the five environments measured 2 ± 0.75 m^2, and differed in enclosure shape and construction material. Rats were allowed to freely explore the enclosure for 2 min, and then placed in the transport cage and moved to the next room (ABCDE), or exited into the hallway and returned to the same room (AAAAA). Following the 5 exposures, rats were carried back to the housing room, rested for 25 min, then sacrificed by transcardial perfusion with 4% PFA solution (described in further detail later). In total, the ABCDE rats were exposed to 13.75 m^2 of area when all novel environments were combined; while AAAAA rats were exposed to 2.75 m^2. This gives a ratio of approximately $x = 5$ when we consider the increased area of space experienced (x in the URDWR model) by the ABCDE versus AAAAA groups (Table 1). *Homer1a* activation analysis was performed to quantify pyramidal cell activation proportions in CA1 and CA3.

MP4: Detailed methods for this study are previously described in the immediate-early gene component of the Alme *et al.* (2010) study. In the published study, behavior-induced *Arc* mRNA expression data were only reported for dentate gyrus. After publication, CA1 and CA3 were subsequently analyzed and are included in the current meta-analysis. Twenty-eight adult (10–12 months) male Fischer-344 rats (Harlan Sprague Dawley, Indianapolis IN) were divided into four experimental groups (Groups 1–4; $n = 5$ each) and two control groups, which included a negative gene expression control group (Groups 5A and 5B; no environmental exposure at test, $n = 5$), and a MECS control group ($n = 3$). On the final Test Exposure day, Groups 1 and 2 were exposed to four different environments (each associated with a different experimenter and transport carrier), and groups 3 and 4 were exposed to one environment four times, before sacrifice by decapitation. The environments consisted of enclosures of various shapes: circular arena (area ~ 0.5 m^2), rectangular arena (~0.6 m^2), an isosceles triangular arena (~0.5 m^2); and a square arena (~0.64 m^2). Experimenters ensured rats traversed the entire space within the enclosure based on grid markings laid down on the floor of the arenas. In total, Groups 1 and 2 were exposed to ~2.24 m^2 of area when all four environments were combined; while groups 3 and 4 rats were exposed to ~0.64 m^2 (the square arena only). This gives a ratio of approximately 3.5, rounded to $x = 4$, when we consider the increased area of space experienced (x in the URDWR model) by Groups 1 and 2 versus Groups 3 and 4 (Table 1). The caged Control Groups (5A, 5B) were sacrificed after being taken directly from their home cages. The exploration time allowed for each rat in each apparatus for Groups 1–4 on the final Test Exposure day was 4 min in duration. Further details of the behavioral procedure is provided in the published paper (Alme et al., 2010). *Arc* activation analysis was performed to quantify activation proportions in CA1 and CA3.

CT5: Data from this study are derived from the adult groups described in Xie, 2013 (MSc Thesis, University of Lethbridge, Xie, 2013). Thirty naive, male Long-Evans rats, 4.5–5.5 months old, were divided into groups consisting of: caged controls (HC, $n = 9$), small track runners (X1, $x = 9$), large track runners (X4, $x = 9$), and positive gene expression control (MECS, $n = 3$). Each rat was trained twice daily for 5 days on a large (0.34 m^2, circumference 343.0 cm) and small (0.09 m^2, circumference 86.1 cm) circular track connected by a 40cm long removable bridge that was the same height and width as the tracks. The ratio of track areas was 4. Photographs of the transport containers and circular tracks are available in Xie (2013). During training, rats were transported from the animal housing room to the experiment room in a covered plastic box. The holding box had opaque walls and limited space for exploration but did not restrict the rat's movement (29.2 cm × 18.7 cm × 15.2 cm). Days 1–3 of training involved a 10 min session twice daily, during which each rat moved between two tracks via the bridge connection and in the clockwise direction on each track. Wooden blocks that could obstruct the track passage were used to help guide the rat to move in the correct direction. Food reward was given at random locations on the track. This free movement between the two tracks ensured that rats became familiar with the two separate locations of each track, which were unchanged throughout training and testing. For days 4–5 of training, the tracks remained in the original configuration and location in the experiment room, but the connecting bridge was removed. Twice daily, each animal ran unidirectionally on one track for 5 min, was carried (uncovered) to the other track, and ran unidirectionally for another 5 min. On test

day, each rat, spent a minimum of 1 hour in a dark box in the testing room prior to behavior, in order to establish baseline *Homer1a* gene expression. Behavioral groups ran for 5 min unidirectionally on either the large circular track (X4, $n = 9$) or small circular track (X1, $n = 9$), then returned to their dark holding box for 24 min before sacrifice by timed transcardial perfusion with 4% PFA solution. HC subjects were directly sacrificed after spending a minimum of 1 hour in the dark box. Positive controls were perfused 25 min post MECS treatment. *Homer1a* activation analysis was performed to quantify subpopulations recruited in X1 versus X4 groups in CA1.

AB6 & AB7 (each detailed below): Rats were exposed to either two different environments (AB) or the same environment twice (AA). Exposures were separated by a 20 min interval in a resting chamber. Double *Homer1a* and *Arc* activation analysis was performed to quantify subpopulation overlap in the A/B versus A/A exposures in CA1 and CA3.

AB6: Six adult (3 months old) naïve, male Long-Evans rats were divided into AB exposure ($n = 4$) and AA exposure ($n = 2$) test groups. Rats were handled twice daily for 10 min for 1 week prior to test day and acclimated to a darkened antechamber in different home-cages for quiescence.

On test day, AA rats were exposed to the same novel room twice. Each exposure was 5 min in duration, separated by a 20 min rest period. AB rats were exposed to two different novel rooms for 5 min each, separated by a 20 min rest period. Rest periods occurred in a darkened antechamber isolated from both of the exposure environments. In room 1 (experienced twice by AA group), rats were placed on a linear track (area = 0.4 m^2). In room 2, rats were placed on a circular track (area = 0.44 m^2). Rats were prodded to explore the entire track in alternating directions. Laps were recorded in each room. In total, the AB group was exposed to 0.84 m^2 of area in the two different environments; while the AA group was exposed to 0.44 m^2 on the linear track. This gives a ratio of 1.9, rounded to $x = 2$, when we consider the increased area of space experienced (x in the URDWR model) by the AB condition versus AA condition. Rats were sacrificed by decapitation after the second exposure.

AB7: Fourteen adult naive, male Long-Evans rats were divided into AB exposure ($n = 8$) and AA exposure ($n = 6$) test groups. All rats tested and reported here received unilateral hippocampal lesions via multiple NMDA injection sites. Prior to behavioural training, rat brains underwent MRI scanning to verify lesions. Rats received extensive training prior to test day. Rats were trained to run down either side of a divided linear track (~76 cm X 40 cm, area = 3040 cm^2) for food reward. Turns were unidirectional. Initial training also involved walking on a long linear track that extended from the hallway to the small linear track. After this, regular AB training occurred such that the track was moved to either of two distinct rooms and rats had to turn in opposite directions in either room. On test day, rats were transported to room 1 in a small dark container and rested in the container for 1 hour. Lights were turned on, and the animal was placed on the track for 10 s to familiarize with the room. Lights were then turned off (except for a dim red light) and rats started track running for 5 min, after which they were placed in the transport container and the lights were turned on again. AA groups rested for 20 min and repeated this in the same room. For the AB group, rats were then transported to room 2 while propped up on the edge

of the container to view the transport route. After resting in the dark room 2 for 20 min, AB subjects were exposed to the track, ran in opposite directions of the track for 5 min. While the AB group was exposed to the same track twice but in two distinct rooms, for the purposes of calculating activation proportions, we will consider the AB rats as having experienced double the area as AA rats. This gives a ratio of $x = 2$, when we consider the increased area of distinct space experienced (x in the URDWR model) by the AB condition versus AA condition. After the second running epoch, all rats were sacrificed by transcardial perfusion with 4% PFA.

Sacrifice and tissue collection—In studies MP1, MP2, MP4 and AB6, rats were guillotine-decapitated under heavy isofluorane anesthesia. Brains were extracted rapidly (within 2–3 min), and then flash frozen directly in cold 2-methylbutane immersed in a slurry of ethanol and dry ice. In studies MP3, CT5, and AB7, rats received injections of sodium pentobarbital (500 mg/kg, i.p.) and were perfused transcardially with 200 ml of phosphate buffered saline (0.1M PBS) followed by 200 ml of 4% paraformaldehyde (PFA) solution. To prevent RNA degradation, all tools were decontaminated with RNAse Away™ (Ambion™, ThermoFisher Scientific), all solutions were prepared with diethyl dicarbonate-treated water (RNases inactivated), and perfusions were tightly timed. Brains were extracted and stored in 4% PFA solution for 2–3 h for post-fixation, transferred to 30% sucrose for cryoprotection, and stored at −80°C until sectioning. For each cohort, brains from different test conditions were included in a single tissue block made with Tissue-Tek ® O.C.T.™ compound (Miles Elkhart, IN or OpticsPlanet, IL) to ensure uniformity of tissue handling and FISH conditions, and then cryo-sectioned at either 20 μm (MP1, MP2, MP4, AB6) or 40 μm (MP3, CT5, AB7) onto SuperFrost-Plus™ microscope slides (VWR or ThermoFisher Scientific).

Fluorescence in situ hybridization—Slides with brain sections representing the various test conditions in each experiment were processed through fluorescence *in situ* hybridization (FISH) to tag intranuclear *Homer1a* (studies MP1, MP2, MP3, CT5) or *Arc* (study MP4) mRNA intranuclear transcription foci. Studies AB6 and AB7 employed dual-IEG catFISH labelling to co-label both *Homer1a* and *Arc*. The exact procedure for *H1a*-FISH performed in studies MP1 and MP2 are previously detailed in Montes-Rodriguez *et al.* (2013). Briefly, fluorescein-labeled *H1a* antisense riboprobes were generated using an *H1a* cDNA clone, directed to the 4.4 kb 3′ UTR. After probe hybridization, fluorescein-tyramide conjugate dye (PerkinElmer) was applied for signal amplication. Nuclei were counterstained with 4′, 6′ diamidino-2phenylindole (DAPI; Sigma-Aldrich). This *H1a*-FISH procedure was also performed in studies MP3 and CT5 with fixed tissue, with the addition of proteinase K buffer digestion after the initial fixation step.

The *Arc*-FISH protocol for MP4 is described in Alme *et al.* (2010). Full-length *Arc* cDNA was used to generate digoxigenin-labeled riboprobes. After hybridization, slides were incubated with digoxigenin antibody conjugated to horseradish peroxidise (HRP), and then detected with a cyanine-3 (CY3) amplification kit (PerkinElmer). Nuclei were counterstained with Sytox-green (Molecular Probes).

General catFISH protocol for AB6 and AB7 is outlined in Vazdarjanova and Guzowski (2004), also with the addition of proteinase K buffer after the first fixation step for AB7 (fixed tissue). Instead of full-length *Arc* probe, AB6 and AB7 used an *Arc* riboprobe that only targeted introns on the *Arc* transcript. Both this intron-only *Arc* probe (DIG labeled) and the 3′UTR *H1a* probe (fluorescein labeled) were applied for overnight hybridization. After quenching, DIG-antibody was applied overnight, followed by TSA-biotin conjugation with Texas Red, which served as two-step signal amplification against the smaller *Arc* probe. After that, fluorescein-dye conjugate was used to amplify *H1a* signal. Nuclei were counterstained with DAPI.

Image acquisition and analysis—Visualization of fluorescent mRNA-labeled brain slices was performed either by laser confocal imaging (MP4, CT5, AB6, AB7) or digital wide-field fluorescence scanning by NanoZoomer (Digital Pathology RS, Hamamatsu Photonics) (MP1, MP2). Study MP3 employed both methods. Since imaging settings such as laser intensity and offset parameters differed between experiments, the general acquisition protocols for studies MP1 and MP2 (Witharana, 2011); MP3 (Cardiff, 2012); CT5 (Xie, 2013) are previously described in the corresponding theses. Image settings for MP4 are included in Alme *et al.* (2010) and details for AB6 and AB7 are described in Montes-Rodriguez *et al.* (2013).

Confocal images for studies MP4, CT5, AB6 and AB7 were analyzed by an automated intranuclear foci (INF) detection plug-in, “IEG-analysis”, developed in-house (by V. Trivedi) for the open software ImageJ (NIH, Bethesda, MD). The exact algorithm for 3D detection and characterization of *Homer1a* and *Arc* INFs is detailed in a published study (Montes-Rodriguez et al., 2013). Image stacks from MP4 were reconstructed with Adobe Photoshop (Adobe Systems, San Jose, CA) to generate two-dimensional images for reference, and then INFs were quantified manually (described in Alme et al., 2010). NanoZoomer images from studies MP1 and MP2, consisting of larger brain areas compared to confocal images, were analyzed by an automated *H1a*-INF detection program written in Visual Basic C++, “GreenDot,” also developed in Lethbridge (by V. Trivedi), the details of which are outlined in Witharana (2011). Confocal and nanozoomer images from MP3 were analyzed through automated *H1a*-INF characterization by a MatLab (The MathWorks Inc., Natick, MA) program (developed by J. Cardiff) and described in Cardiff (2012).

In general, to maintain within-slide consistency of image acquisition parameters, the MECS brain on each slide was typically imaged first at the beginning of the scanning of each slide, and the settings such as laser intensity or laser dwell time, were determined from this image sample. For confocal images, the imaging software provided an intensity histogram so the experimenter could then adjust the laser intensity in the appropriate channel to give about 5% saturation of intranuclear foci in the MECS sample, thus covering as much of the dynamic range as possible. Similarly, for NanoZoomer images, after acquisition, the sample MECS image was viewed in a separate program (ImageJ) that outputted a fluorescence intensity/saturation histogram. The fluorescent light settings were then adjusted to permit about 5% saturation of intranuclear foci, and minimal out-of-focus rings (from out-of-plane signals because of epifluorescence acquisition).

Electrophysiological Studies

Behavioral procedures

Circle track ensemble recording: Maurer *et al.* (2006) recorded neural activity in dorsal and middle hippocampal CA1 while rats ran unidirectionally on a small track (167.5 cm); and bidirectionally on a large track (382 cm). Rats ran for two 20 min sessions a day, once on the large circle and once on the small circle (counterbalanced), resulting in variable laps per day. The tracks were located concentrically in the recording theater, and the rats rested/slept on a platform at the middle (the small track was removed during rest to prevent animals from accessing it).The nested two-track arrangement was used to increase the yield of independent place fields during recording, but also coincidentally resembles the paradigm used in IEG study CT5. Further details regarding the behavioral methods are provided in the published paper. For the purposes of this current paper, the numbers of place fields observed on the tracks were reanalysed to compute the expected activation ratio for the large (P_x) and small track (P_1) under the assumption of URDWR, then compared with the observed ratios. The ratio of track diameters was 2.3:1, ($x = 2.3$ in the URDWR model); however, since the animals ran in both directions on the large track, and because place fields in the opposite running direction are largely uncorrelated when the animals are experienced with the bidirectional running (McNaughton et al., 1983; Navratilova et al., 2012), we computed the expected activation ratios for track ratios of both 2.3:1 ($x = 2.3$) and twice that 4.6:1 ($x = 4.6$).

MULTIPLE–PLACE ENSEMBLE RECORDING

Alme *et al.* (2014) recently recorded CA3 ensemble activity in 11 different enclosures (one familiar; 10 novel), each situated in a different room to determine whether firing patterns overlapped in the 55 place-map comparisons. This massed exposure paradigm is a procedural extension of our multiple-place IEG studies and thus we include their published activation ratios for comparison. During tetrode positioning, rats were familiarized with a black square box (100 × 100 × 50 cm) that contained chocolate sprinkles. During testing, the authors used a mobile recording trolley to sustain spike recording during transport between the different rooms. On day one of testing, rats were exposed to the familiar room, then to five novel rooms, and then returned to the familiar room. On the second day of testing, rats were exposed to the five other novel rooms, flanked again with the familiar room at the beginning and end of the recordings. On both days, subjects were exposed twice to one of the five novel rooms for firing pattern analysis. The rat enclosures were all square black boxes that measured 100 × 100 × 50 cm, except for one box that measured 100 × 100 × 80 cm. In all rooms, rats foraged for food morsels in these recording boxes. Further details regarding the behavioral methods are provided in the published paper. For the purposes of this current paper, the activation proportions across the different rooms were extracted from the results presented in Alme *et al.* (2014) and converted to URDWR-expected and observed ratios. In total, rats were exposed to 11 different boxes measuring 100 cm × 100 cm. This gives a ratio of $x = 11$ when we consider the increased area of novel space experienced (x in the URDWR model) when compared to activation in only the familiar or training box (also measured 100 cm X 100 cm).

RESULTS

IEG Studies

For the seven IEG experiments reported here, the total activated neurons for x units of area (ratio of total area experienced by multi-environment group versus single-environment group) was compared to the expected total given URDWR and an estimate of P_1 (Table 1). The IEG experiments differed in several possibly critical details, including relative total areas of space to which the animals were exposed, the person who actually conducted the experiments, the animal strain, whether the animals were transported between multiple environments in a covered or uncovered transport box, whether the animals had a long or short period of rest between exposures to different environments, and whether or not the environments were familiar. In addition, there were differences in the way that imaging and image analysis were carried out (see methods). Some experiments used confocal imaging with a photomultiplier setting adjusted by eye on sections from animals that were sacrificed from home cage resting conditions (in which IEG expression is typically very weak) and then held constant across a given slide for other conditions. Confocal images were typically analysed by manual counting of IEG positive cells. Others studies used a NanoZoomer wide-field fluorescence slide scanner to sample large numbers of cells, and automated segmentation and quantification of IEG intranuclear transcription foci. Finally, some analyses included subtraction of relative counts obtained from home cage rest conditions while others used uncorrected scores. We consider these technical dissimilarities and the issue of threshold setting in greater depth below.

Despite these methodological differences, there was a substantial under-recruitment of IEG positive neurons compared to URDWR in all seven IEG experiments. This under-recruitment was consistent across subfields CA1, CA3 and dorsal subiculum. Detailed activation measures are outlined in Table 1.

Electrophysiological Recording

A total of 667 dorsal CA1 pyramidal cells and 535 middle CA1 pyramidal cells (from three rats) were included in the analysis. Data from this study consisted of both mean firing rate for each neuron in each epoch, as well as the number of discrete place fields. Place fields were defined using the criterion of a single cycle of phase precession as described in the original published report. We used the numbers of place fields observed on the small track to compute the expected activation ratio for the large and small tracks. If a cell had one or more fields, it was considered activated. The ratio of track diameters was 2.3:1; however, since the animals ran in both directions on the large track, and because place fields in the opposite running direction are largely uncorrelated when the animals are experienced with the bidirectional running (McNaughton et al., 1983; Navratilova et al., 2012), we computed the expected activation ratios for track ratios of both 2.3:1 and twice that (4.6:1). In both cases, the observed activation ratios considerably underestimated the ratios predicted by URDWR (Fig. 3A). In addition, the number of fields per cell expressed between the two tracks was significantly correlated (r (dorsal hippocampus) = 0.50 ($P < 10^{-7}$); r (middle hippo-campus) = 0.39 ($P < 10^{-7}$), indicating that the selection probability was not uniform in

the population. Finally, the frequency distribution of the number of fields per cell was highly positively skewed, and deviated substantially from the Poisson prediction (Fig. 3D).

The mean firing rates for pre-track sleep and track running were 1.0 Hz and 1.3 Hz for dorsal hippocampus, and 1.1 Hz and 1.4 Hz for middle hippocampus. Irrespective of place fields, the overall firing rates for the two tracks were quite highly correlated for both the dorsal cells ($r = 0.729$; $P < 10^{-7}$) and middle cells ($r = 0.637$; $P < 10^{-7}$). In addition, the firing rates in the pre-track sleep epochs were significantly correlated with the mean firing rates on the large and small tracks for both the dorsal ($r = 0.612$; $P < 10^{-7}$) and middle ($r = 0.314$; $P < 10^{-7}$), indicating that about 38% and 10% respectively of the firing rate variance on the tracks can be explained by the rates during sleep prior to experiencing the track on that day, similar to that observed in Rich *et al.* (2014). Note, that the animals were well familiarized with the track, and slept on a platform located at the center of the two circular tracks. These facts could potentially influence the correlations. Nevertheless, the overall conclusion from this analysis is that the firing rates on the two tracks were much more highly correlated than predicted by chance, and that a substantial portion of the firing rate variance on the tracks could be predicted from the rates during sleep (especially for dorsal hippocampus).

For further comparison, we computed activation ratios from two additional neural recording studies. Alme *et al.* (2014) recorded CA3 neurons in a base environment and in 10 additional environments in 10 different rooms. Their results follow the same pattern of underestimation by URDWR, such that the total number of active cells is not predicted by a Poisson distribution. Instead, different cells do possess different activation probabilities (see Results, Alme et al., 2014). Finally, we note that, while the present manuscript was in preparation, Rich *et al.* (2014) provided a detailed analysis of the activation statistics of CA1 cells recorded while rats ran on a 48 m track. They showed that, whereas the locations of firing for individual cells are well described by a Poisson process, the Poisson rate parameters differed widely across cells in the population. The Poisson rate of field formation parameter was well described by a gamma distribution. Their Figure 3C (Rich et al., 2014, pp816) provides a means of estimating the deviation of total number of activated cells from the URWDR (equal Poisson) distribution as environment size increases. The cumulative gamma-Poisson distribution consistently undershoots the cumulative Poisson distribution (URDWR). It is worth noting also, that the degree of undershoot is smaller for small track lengths that are more comparable to typical tracks or environments used for most recording or IEG studies. For example the ratios of the cumulative activation plots is about 1.2 for 5 m tracks and reaches about 1.55 for 30 m track length. These deviations are likely to be underestimates because there was likely a large fraction of cells that were not included in estimating the population parameters because, as discussed above, they never fired enough spikes to form a detectable cluster (see next section and Henze et al., 2000).

Issue of Thresholding and Background Subtraction in IEG Studies

Although most IEG studies have reported results in terms of the number of IEG positive nuclei, based on the presence or absence of INFs detected by a human observer, it is clear that INFs are not all-or-nothing entities. This can be seen in Figure 4, which illustrates the

wide range of INF sizes and brightnesses that would be counted as positive by a human observer and were detected by the automated INF counting algorithms used in some of the studies reported here. As mentioned above, most prior IEG studies have used the approach of adjusting the imaging parameters by eye, which (as will be seen below) likely excludes many very small/dim foci. In some studies reported here, however, imaging parameters were adjusted for maximal sensitivity with minimal saturation in the brightest foci (by using a preliminary image of the MECS control brain per slide to determine consistent imaging settings, see p.8). We used an automated counting algorithm which segmented INFs on the basis of criteria which included number of adjacent pixels above a fixed intensity threshold, and a shape parameter which had to be fulfilled in more than one adjacent image plane. An additional criterion of requiring the detected INF to be on a blue background rejected extranuclear noise. We then integrated the pixel intensity over the segmented INFs and constructed relative frequency histograms for each experimental condition (home cage, one-environment (1E), five-environments (5E), and maximal electroconvulsive shock [MECS]). These histograms are illustrated in Figure 5.

Figure 5 illustrates the problem with setting an imaging threshold for counting INFs. Whereas the HC distribution is unimodal on a log scale, the distributions after exploration tend towards bimodality and predominantly reflect a shift of neurons from a weak IEG expressing pool to a more strongly expressing pool. This is seen as a progressive reduction in the low-intensity mode and a progressive increase and right-shift in the high-intensity mode. Thus, whereas not performing any “background count” subtraction overestimates the true fraction of neurons “activated” by the experimental manipulation, merely subtracting the HC counts from the “experimental” counts underestimates this fraction. Moreover, exposure to multiple environments (or larger ones) leads to the expression of more place fields per cell, which results in more total firing and presumably a consequent increase in IEG expression. This would lead to the right-shift of the high-intensity modes seen in Figure 5. It is clear that setting a relatively high detection threshold could lead to a substantial error in the estimation of the relative total recruitment in small and larger environments such that the observed activation might equal or even exceed the URDWR expectation (depending on where the threshold is set).

To attempt to solve the foregoing issues we developed the following analytical procedure. Using the relative frequency distributions for INF integrated intensity, we found the peak location of the HC distribution and then scaled the HC distribution so that it matched the 1E and 5E distributions at the peak location. These scaled HC distributions provided estimates of the low-intensity mode contained in the 1E and 5E distributions, which were then subtracted out. The residual distributions after subtraction are shown as dotted lines in Figure 5. These residual distributions were integrated and the result multiplied by the relative count values such as in Figure 6. This procedure produces an estimate of the true fraction of neurons “activated” in the 1E and 5E conditions. The results for two such analyses (studies MP1 and MP2) are shown in Table 2.

DISCUSSION

Data from seven different studies using IEG transcription analysis consistently showed under-recruitment of IEG-expressing cells as the total experienced area increased, compared to recruitment levels predicted by the uniform random draw with replacement (URDWR) hypothesis of place cell allocation. The same pattern of results was observed in previously published ensemble recording data from Maurer *et al.* (2006) and Alme *et al.* (2014). In addition, firing rate and place field numbers per cell in recording studies are highly positively skewed, deviating strongly from the uniform Poisson prediction, and this positive skew is mirrored in the skew of the distribution of IEG intranuclear transcription foci integrated intensities. Although the stoichiometry between number of spikes fired and the INF intensity is not known (and may vary regionally and under different brain-states and levels of experience), it is clear from the comparison of the home-cage and MECS distributions that INF intensity does increase with activation levels, and an exploration-induced increase in INF intensity above home-cage levels was previously demonstrated (Miyashita et al., 2009). It has also been shown (Guzowski et al., 2006) that as few as four rounds of behavior in the same environment separated by 30 min substantially suppressed the *Arc* transcriptional response of active neurons without suppressing place cell firing *per se*. However, this dynamic in the electrotranscriptional coupling cannot easily account for the consistent under-recruitment of new neurons as environmental area (or number) increases over time intervals too short for the loss of signal from the earliest neurons activated in the series, which was the case in these studies.

We note that there appears to be an outlier in Figure 1, corresponding to data from Alme *et al.*, (2014). However, this data point lies further from the main cluster only because they recorded in a comparably high number of environments (11 places) so the P_x/P_1 ratio will be high as well. Despite this relatively large number of environments visited, the estimated ratio still falls well below the line of expected values as would be predicted by URDWR. Moreover, as shown by the P_x/P_1 ratio curves in Figure 1, the degree of over–estimation by URDWR of actual activation is related to the intrinsic sparsity of the network under consideration. For example: if one follows one of the curves, it is clear that when P_1 is very small, then the overestimation appears very large whereas if P_1 is quite large to begin with (as would be the case if either the general population was more excitable, or a very large environment was used to estimate P_1) then the degree of overestimation would not appear so large., Thus, the data of Alme *et al.* (2014) are not actually an exception, it is just that they recorded in CA3 (which has intrinsically relatively sparse activity) and used a lot of environments in comparison to the other studies.

Thus, both electrophysiological studies and IEG activation data converge on the conclusion that all four subdivisions of the hippocampus (dentate gyrus [DG], CA3, CA1, and dorsal subiculum [DS]) have highly positively skewed propensities for a given neuron to become activated at a given location. Consistent with electrophysiology, the proportions of neurons activated in a given small environment increases systematically from DG to CA3 to CA1. Averaging the results for experiments MP1 and MP2 gives activation levels of 0.02, 0.06, and 0.18 respectively for an environment of about 60 × 60 cm. Our data did not reveal an additional increase from CA1 to dorsal subiculum. It should be noted, however, that our

estimated activation levels for studies MP1 and MP2 are about half the values estimated either from previous electrophysiology or IEG studies, and closer to the conclusion of Henze *et al.* (2000) who estimated that only about 6–10% of all CA1 cells is activated in a "typical" behavioral condition *in vivo*. In agreement with this general conclusion, the maximal ratio of the equal Poisson (URDWR) and gamma-Poisson distributions for CA1 in the Rich *et al.* (2014) study was about 1.5, whereas in our studies the mean for CA1 (MP1 & MP2) was about 2.5. This suggests that the lowest end of the distribution in the Rich *et al.* study was seriously underestimated because of the large fraction of cells with activity too low to detect in their study, but which are detected with IEG methods. Furthermore, while most data presented in this meta-analysis are derived from activity patterns in dorsal hippocampal regions, we anticipate similar nonuniform recruitment probabilities in intermediate and ventral hippocampal areas given the increased sparsity of place fields in ventral regions. In support of this, Beer *et al.* (2014) demonstrated that the number of *Arc* + neurons declines along the dorso-ventral axis after a behavioral task.

Our estimate for CA1 is very close to the estimate of the proportion of CA1 cells with "place fields" derived from recent *in vivo* Ca^{++} imaging studies in mice (Ziv et al., 2013); however the species and experimental condition differences make the comparison somewhat tenuous. In addition, it should be noted that even optical imaging studies are subject to certain thresholding constraints with respect to calculating "activity" statistics. For example, over 90% of cells in the Ziv *et al.* (2013) study exhibited at least one Ca^{++} transient during running, whereas only ~ 15% had above criterion "place fields". It is possible that some of the transients occurred during sharp-wave-ripples which are not easily detected in imaging studies due to the slow kinetics of the calcium buffer. Nevertheless, Ca^{++} imaging, particularly with more sensitive reporters, will likely yield better estimates of true population firing statistics, particularly since the same cells can be identified with greater certainty over longer periods than extracellular recording. Direct voltage recording using genetically encoded voltage sensors are also expected to yield more accurate results.

One potentially interesting observation that arose during this meta-analysis was that in some studies, the proportions of IEG-marked cells in home-cage groups were actually higher than behavioral groups. We noted this previously in the interpretations of Figures 5 and 6 as it is possible that this phenomenon has important implications for using home-cage counts as a baseline. However, at the time that this meta-analysis was completed, this issue has not been fully resolved in the current literature and for our purposes, we simply used the observed fraction of cells activated by a particular experience as we need a reasonable background subtraction. Speculatively, these high home-cage counts may be related to burst episodes during sleep while the animals were resting. Alternatively, it is possible that the coupling between action potentials and transcription may vary according to brain/neuromodulator states. For example, removing the septal cholinergic projection to the hippocampus does not prevent the cells from firing, but does strong suppress IEG expression (Miyashita et al., 2009). While these are possibilities, further directed research will be required in this field to concretely address these high home-cage activation proportions.

Several mechanisms might underlie the non-uniformity of activation probability among hippocampal cells: intrinsic pre-selection during network development (Epsztein et al.,

2011; Xu et al., 2014), pre-experience rest network reset, or spontaneous dominance and ongoing perpetuation of allocation. It is possible that a limited group of place cells exhibit preferential selection, or higher relative activation probabilities across changing place codes, as a result of plasticity-related hysteresis from past co-activation (Yassin et al., 2010). The exact mechanisms of pre-selection are not known at this point but pre-configured networks and/or intrinsic excitability differences may result in “pre-play” of temporal sequences in primed place cell assemblies (Dragoi and Tonegawa, 2011; Dragoi and Tonegawa, 2013). It is also possible that during a rest period prior to a novel or familiar environmental exposure, a neuronal network with pre-existing synaptic connections is available for upcoming place representations, and these neurons possess a higher probability of activation than those excluded from this selective network. Thus, before a novel place exposure, the rest period might permit a “reset” of the network to participate in the subsequent epochs. Previous studies have reported overlapping populations replayed during a rest period both before and between place exposures (Marrone et al., 2008). Lastly, it is possible that during the experience itself, a group of place units spontaneously gain “dominance” over the place code and this superiority is perpetuated and strengthened throughout the exposure. Rich *et al.* (2014) describe a “cumulative advantage mechanism” similar to this proposed hypothesis. Such a mechanism seems unlikely, however, as it predicts increased skewness of the distribution with experience. Neither the mean firing rates nor the between cell variance changes between post-natal day 16 and adulthood (Langston et al., 2010; Wills et al., 2010), nor between 12 and 24 months of age (Markus et al., 1994; Barnes et al., 1997).

The finding that place cell allocation reflects a nonuniform probability distribution does not necessarily invalidate previous IEG and recording data that describe clear “global remapping” in which place codes appear to “orthogonalize” between various environments (Vazdarjanova and Guzowski, 2004; Leutgeb et al., 2005; Leutgeb et al., 2007; Alme et al., 2014). First, as shown by Rich *et al.* (2014; their Fig. 3C), the difference between the equal Poisson (URDWR and gamma-Poisson distributions becomes smaller as environmental size is reduced. At the typical size of experimental environments, there is still a substantial fraction of cells that are active in one environment and silent in a second, as they show in their Figure 4. Second, even when cells have fields in two environments (or multiple fields in a single large environment), the apparently random allocation of fields to position ensures that the fields of two cells that overlap in one location are unlikely to do so in another, ensuring a high degree of location/environment discrimination by the population. Finally, the possibility that the activation propensity of hippocampal neurons (and possibly neurons in other regions as well) is stochastic over time must be considered. In studies in which multiple experiences occur within a narrow time window, as most of the studies reported here, and as in most recording studies, it might be the case that having fired in one context predisposes a cell to fire again a short time later in a different context; however, Rich *et al.* (2014) show fairly conclusively that this is not the case since the recruitment was “memoryless”. An alternative possibility is that neurons express some stochastic factor, such as, for example CREB (Han et al., 2007) that modulates their excitability over some time window. This would provide a mechanism by which hippocampal representations of two events that are time separated would be more orthogonal than if the events were experienced in closer temporal proximity. Future studies will be required to explore this possibility.

Skewed hippocampal activation distributions are consistent with a nonuniform recruitment strategy that also exists in other sensory systems such as auditory (Hromádka et al., 2008) and whisker barrel cortex (O'Connor et al., 2010). Log-normal recruitment seems to be a recurring feature of brain networks and pervades all levels of sensory processing (Buzsáki and Mizuseki, 2014). The skewed distribution of the probability of a given cell having place fields in the hippocampus may enhance coding capacity and flexibility, and may have critical significance for episodic memory formation and retrieval.

Acknowledgments

NIH MH046823 (BLM), Alberta Innovates-Health Solutions Polaris Award (BLM), Natural Sciences and Engineering Council of Canada 418422 & 429438 (BLM), McKnight Brain Research Foundation (CAB), NIH R03AG049411 (APM), Canadian Institutes of Health Research 106711 (RJS), NSF IOS 1026046 (JFG), and Funds from James L. McGaugh Chair in the Neurobiology of Learning and Memory (JFG).

References

Alme CB, Buzzetti R, Marrone D, Leutgeb J, Chawla M, Schaner M, Bohanick J, Khoboko T, Leutgeb S, Moser E. 2010; Hippocampal granule cells opt for early retirement. Hippocampus. 20: 1109–1123. [PubMed: 20872737]

Alme CB, Miao C, Jezek K, Treves A, Moser EI, Moser MB. 2014; Place cells in the hippocampus: Eleven maps for eleven rooms. Proc Natl Acad Sci. 111: 18428–18435. [PubMed: 25489089]

Barnes CA, McNaughton BL, Mizumori SJ, Leonard BW, Lin L-H. 1990; Comparison of spatial and temporal characteristics of neuronal activity in sequential stages of hippocampal processing. Prog Brain Res. 83: 287–300. [PubMed: 2392566]

Barnes CA, Suster M, Shen J, McNaughton BL. 1997; Multistability of cognitive maps in the hippocampus of old rats. Nature. 388: 272–275. [PubMed: 9230435]

Beer Z, Chwiesko C, Sauvage MM. 2014; Processing of spatial and non-spatial information reveals functional homogeneity along the dorso-ventral axis of CA3, but not CA1. Learn Memory. 111: 56–64.

Bostock E, Muller RU, Kubie JL. 1991; Experience-dependent modifications of hippocampal place cell firing. Hippocampus. 1: 193–205. [PubMed: 1669293]

Bottai D, Guzowski JF, Schwarz MK, Hang SH, Xiao B, Lanahan A, Worley PF, Seeburg PH. 2002; Synaptic-activity induced conversion of intronic to extronic sequence in Homer 1 immediate early gene expression. J Neurosci. 22: 167–175. [PubMed: 11756499]

Burke SN, Chawla MK, Penner MR, Crowell BE, Worley PF, Barnes CA, McNaughton BL. 2005; Differential encoding of behavior and spatial context in deep and superficial layers of the neocortex. Neuron. 45: 667–674. [PubMed: 15748843]

Burke SN, Maurer AP, Nematollahi S, Uprety AR, Wallace JL, Barnes CA. 2011; The influence of objects on place field expression and size in distal hippocampal CA1. Hippocampus. 21: 783–801. [PubMed: 21365714]

Buzsáki G, Mizuseki K. 2014; The log-dynamic brain: how skewed distributions affect network operations. Nat Rev Neurosci. 14: 264–278.

Cardiff, J. Experienced-induced immediate early gene expression in hippocampus after granule cell loss. Master of Science, University of Lethbridge; 2012.

Chawla MK, Guzowski JF, Ramirez-Amaya V, Lipa P, Hoffman KL, Marriott LK, Worley PF, McNaughton BL, Barnes CA. 2005; Sparse, environmentally selective expression of Arc RNA in the upper blade of the rodent fascia dentata by brief spatial experience. Hippocampus. 15: 579–586. [PubMed: 15920719]

Deguchi Y, Donato F, Galimberti I, Cabuy E, Caroni P. 2011; Temporally matched subpopulations of selectively interconnected principal neurons in the hippocampus. Nat Neurosci. 14: 495–504. [PubMed: 21358645]

Dragoi G, Tonegawa S. 2011; Preplay of future place cell sequences by hippocampal cellular assemblies. Nature. 469: 397–401. [PubMed: 21179088]

Dragoi G, Tonegawa S. 2013; Distinct preplay of multiple novel spatial experiences in the rat. Proc Natl Acad Sci. 110: 9100–9105. [PubMed: 23671088]

Epsztein J, Brecht M, Lee AK. 2011; Intracellular determinants of hippocampal CA1 place and silent cell activity in a novel environment. Neuron. 70: 109–120. [PubMed: 21482360]

Frank LM, Stanley GB, Brown EN. 2004; Hippocampal plasticity across multiple days of exposure to novel environments. J Neurosci. 24: 7681–7689. [PubMed: 15342735]

Guzowski JF, Lyford GL, Stevenson GD, Houston FP, McGaugh JL, Worley PF, Barnes CA. 2000. Inhibition of activity-dependent Arc protein expression in the rat hippocampus impairs the maintenance of long-term potentiation and the consolidation of long-term memory. J Neurosci. 3993–4001. [PubMed: 10818134]

Guzowski JF, McNaughton BL, Barnes CA, Worley PF. 1999; Environment-specific expression of the immediate-early gene Arc in hippocampal neuronal ensembles. Nat Neurosci. 2: 1120–1124. [PubMed: 10570490]

Guzowski JF, Miyashita T, Chawla MK, Sanderson J, Maes LI, Houston FP, Lipa P, McNaughton BL, Worley PF, Barnes CA. 2006; Recent behavioral history modifies coupling between cell activity and Arc gene transcription in hippocampal CA1 neurons. Proceedings of the National Academy of Sciences of the United States of America. 103: 1077–1082. [PubMed: 16415163]

Guzowski JF, Timlin JA, Roysam B, McNaughton BL, Worley PF, Barnes CA. 2005; Mapping behaviorally relevant neural circuits with immediate-early gene expression. Curr Opin Neurobiol. 15: 599–606. [PubMed: 16150584]

Hafting T, Fyhn M, Molden S, Moser M-B, Moser EI. 2005; Microstructure of a spatial map in the entorhinal cortex. Nature. 436: 801–806. [PubMed: 15965463]

Han J-H, Kushner SA, Yiu AP, Cole CJ, Matynia A, Brown RA, Neve RL, Guzowski JF, Silva AJ, Josselyn SA. 2007; Neuronal competition and selection during memory formation. Science. 316: 457–460. [PubMed: 17446403]

Henze DA, Borhegyi Z, Csicsvari J, Mamiya A, Harris KD, Buzsáki G. 2000; Intracellular features predicted by extracellular recordings in the hippocampus in vivo. J Neurophysiol. 84: 390–400. [PubMed: 10899213]

Hill AJ. 1978; First occurrence of hippocampal spatial firing in a new environment. Exp Neurol. 62: 282–297. [PubMed: 729680]

Hromádka T, DeWeese MR, Zador AM. 2008; Sparse representation of sounds in the unanesthetized auditory cortex. PLoS Biol. 6: 10–1371.

Jung MW, Wiener SI, McNaughton BL. 1994; Comparison of spatial firing characteristics of units in dorsal and ventral hippocampus of the rat. J Neurosci. 14: 7347–7356. [PubMed: 7996180]

Kjelstrup KB, Solstad T, Brun VH, Hafting T, Leutgeb S, Witter MP, Moser EI, Moser M-B. 2008; Finite scale of spatial representation in the hippocampus. Science. 321: 140–143. [PubMed: 18599792]

Langston RF, Ainge JA, Couey JJ, Canto CB, Bjerknes TL, Witter MP, Moser EI, Moser MB. 2010; Development of the spatial representation system in the rat. Science. 328: 1576–1580. [PubMed: 20558721]

Lee D, Lin B-J, Lee AK. 2012; Hippocampal place fields emerge upon single-cell manipulation of excitability during behavior. Science. 337: 849–853. [PubMed: 22904011]

Leutgeb JK, Leutgeb S, Moser M-B, Moser EI. 2007; Pattern separation in the dentate gyrus and CA3 of the hippocampus. Science. 315: 961–966. [PubMed: 17303747]

Leutgeb S, Leutgeb JK, Barnes CA, Moser EI, McNaughton BL, Moser M-B. 2005; Independent codes for spatial and episodic memory in hippocampal neuronal ensembles. Science. 309: 619–623. [PubMed: 16040709]

Mankin EA, Sparks FT, Slayyeh B, Sutherland RJ, Leutgeb S, Leutgeb JK. 2012; Neuronal code for extended time in the hippocampus. Proc Natl Acad Sci. 109: 19462–19467. [PubMed: 23132944]

Mankin EA, Diehl GW, Sparks FT, Leutgeb S, Leutgeb JK. 2015; Hippocampal CA2 activity patterns change over time to a larger extent than between spatial contexts. Neuron. 85: 190–201. [PubMed: 25569350]

Markus EJ, Barnes CA, McNaughton BL, Gladden VL, Skaggs W. 1994; Spatial information content and reliability of hippocampal CA1 neurons: effects of visual input. Hippocampus. 4: 410–421. [PubMed: 7874233]

Marr D. 1971. Simple memory: a theory for archicortex. Philos T Roy Soc B. 23–81.

Marrone DF, Satvat E, Odintsova IV, Gheidi A. 2014; Dissociation of spatial representations within hippocampal region CA3. Hippocampus. 24: 1417–1420. [PubMed: 25220839]

Marrone DF, Schaner MJ, McNaughton BL, Worley PF, Barnes CA. 2008; Immediate-early gene expression at rest recapitulates recent experience. J Neurosci. 28: 1030–1033. [PubMed: 18234881]

Maurer AP, Cowen SL, Burke SN, Barnes CA, McNaughton BL. 2006; Organization of hippocampal cell assemblies based on theta phase precession. Hippocampus. 16: 785–794. [PubMed: 16921501]

Maurer AP, VanRhoads SR, Sutherland GR, Lipa P, McNaughton BL. 2005; Self-motion and the origin of differential spatial scaling along the septo-temporal axis of the hippocampus. Hippocampus. 15: 841–852. [PubMed: 16145692]

McNaughton BL, Barnes CA, Gerrard JL, Gothard K, Jung MW, Knierim JJ, Kudrimoti H, Qin Y, Skaggs WE, Suster M. 1996; Deciphering the hippocampal polyglot: the hippocampus as a path integration system. J Exp Biol. 199: 173–185. [PubMed: 8576689]

McNaughton BL, Barnes CA, O';Keefe J. 1983; The contributions of position, direction, and velocity to single unit activity in the hippocampus of freely-moving rats. Exp Brain Res. 52: 41–49. [PubMed: 6628596]

McNaughton, BL, Nadel, L. Hebb-Marr networks and the neurobiological representation of action in space Neuroscience and connectionist theory MA Gluck and DE Rumelhart. Hillsdale, NJ: Lawrence Erlbaum; 1990. 1–63.

Miyashita T, Kubik S, Haghighi N, Steward O, Guzowski JF. 2009; Rapid activation of plasticity-associated gene transcription in hippocampal neurons provides a mechanism for encoding of one-trial experience. J Neurosci. 29: 898–906. [PubMed: 19176799]

Mizuseki K, Buzsáki G. 2013; Preconfigured, skewed distribution of firing rates in the hippocampus and entorhinal cortex. Cell Rep. 4: 1010–1021. [PubMed: 23994479]

Monaco JD, Rao G, Roth ED, Knierim JJ. 2014; Attentive scanning behavior drives one-trial potentiation of hippocampal place fields. Nat Neurosci. 17: 725–31. [PubMed: 24686786]

Montes-Rodriguez CJ, Lapointe V, Trivedi V, Lu Q, Demchuk AM, McNaughton BL. 2013; Postnatal development of Homer1a in the rat hippocampus. Hippocampus. 23: 890–902. [PubMed: 23733398]

Navratilova Z, Hoang LT, Schwindel CD, Tatsuno M, McNaughton BL. 2012; Experience-dependent firing rate remapping generates directional selectivity in hippocampal place cells. Front Neural Circuit. 6: 6. doi: 10.3389/fncir.2012.00006

O'Connor DH, Peron SP, Huber D, Svoboda K. 2010; Neural activity in barrel cortex underlying vibrissa-based object localization in mice. Neuron. 67: 1048–1061. [PubMed: 20869600]

O'Keefe J, Dostrovsky J. 1971; The hippocampus as a spatial map. Preliminary evidence from unit activity in the freely-moving rat. Brain Res. 34: 171–175. [PubMed: 5124915]

O'Keefe, J, Nadel, L. The hippocampus as a cognitive map. Oxford: Clarendon Press; 1978.

O'Reilly RC, McClelland JL. 1994; Hippocampal conjunctive encoding, storage, and recall: avoiding a trade-off. Hippocampus. 4: 661–682. [PubMed: 7704110]

Park E, Dvorak D, Fenton AA. 2011; Ensemble place codes in hippocampus: CA1, CA3, and dentate gyrus place cells have multiple place fields in large environments. PloS One. 6: 10–1371.

Rich PD, Liaw HP, Lee AK. 2014; Large environments reveal the statistical structure governing hippocampal representations. Science. 345: 814–7. [PubMed: 25124440]

Rosi S, Ramirez-Amaya V, Vazdarjanova A, Esparza EE, Larkin PB, Rike JR, Wenk GL, Barnes CA. 2009; Accuracy of hippocampal network activity is disrupted by neuroinflammation: rescue by memantine. Brain. 132: 2464–2477. [PubMed: 19531533]

Samsonovich A, McNaughton BL. 1997; Path integration and cognitive mapping in a continuous attractor neural network model. J Neurosci. 17: 5900–5920. [PubMed: 9221787]

Shen J, Barnes CA, McNaughton BL, Skaggs WE, Weaver KL. 1997; The effect of aging on experience-dependent plasticity of hippocampal place cells. J Neurosci. 17: 6769–6782. [PubMed: 9254688]

Thompson L, Best P. 1989; Place cells and silent cells in the hippocampus of freely-behaving rats. J Neurosci. 9: 2382–2390. [PubMed: 2746333]

Thompson L, Best P. 1990; Long-term stability of the place-field activity of single units recorded from the dorsal hippocampus of freely behaving rats. Brain Res. 509: 299–308. [PubMed: 2322825]

Treves A, Rolls ET. 1992; Computational constraints suggest the need for two distinct input systems to the hippocampal CA3 network. Hippocampus. 2: 189–199. [PubMed: 1308182]

Vazdarjanova A, Guzowski JF. 2004; Differences in hippocampal neuronal population responses to modifications of an environmental context: evidence for distinct, yet complementary, functions of CA3 and CA1 ensembles. J Neurosci. 24: 6489–6496. [PubMed: 15269259]

Wills TJ, Cacucci F, Burgess N, O'Keefe J. 2010; Development of the hippocampal cognitive map in preweanling rats. Science. 328: 1573–1576. [PubMed: 20558720]

Wilson MA, McNaughton BL. 1993; Dynamics of hippocampal ensemble code for space. Science. 261: 1055–1058. [PubMed: 8351520]

Witharana, WKL. Non-Boolean characterization of Homer1a intranuclear transcription foci. Master of Science, University of Lethbridge; 2011.

Xie, JY. The effect of development on spatial pattern separation in the hippocampus as quantified by the Homer1a immediate-early gene. Master of Science, University of Lethbridge; 2013.

Xu H-T, Han Z, Gao P, He S, Li Z, Shi W, Kodish O, Shao W, Brown KN, Huang K. 2014; Distinct lineage-dependent structural and functional organization of the hippocampus. Cell. 157: 1552–1564. [PubMed: 24949968]

Yassin L, Benedetti BL, Jouhanneau J-S, Wen JA, Poulet JF, Barth AL. 2010; An embedded subnetwork of highly active neurons in the neocortex. Neuron. 68: 1043–1050. [PubMed: 21172607]

Ziv Y, Burns LD, Cocker ED, Hamel EO, Ghosh KK, Kitch LJ, El Gamal A, Schnitzer MJ. 2013; Long-term dynamics of CA1 hippocampal place codes. Nat Neurosci. 16: 264–6. [PubMed: 23396101]

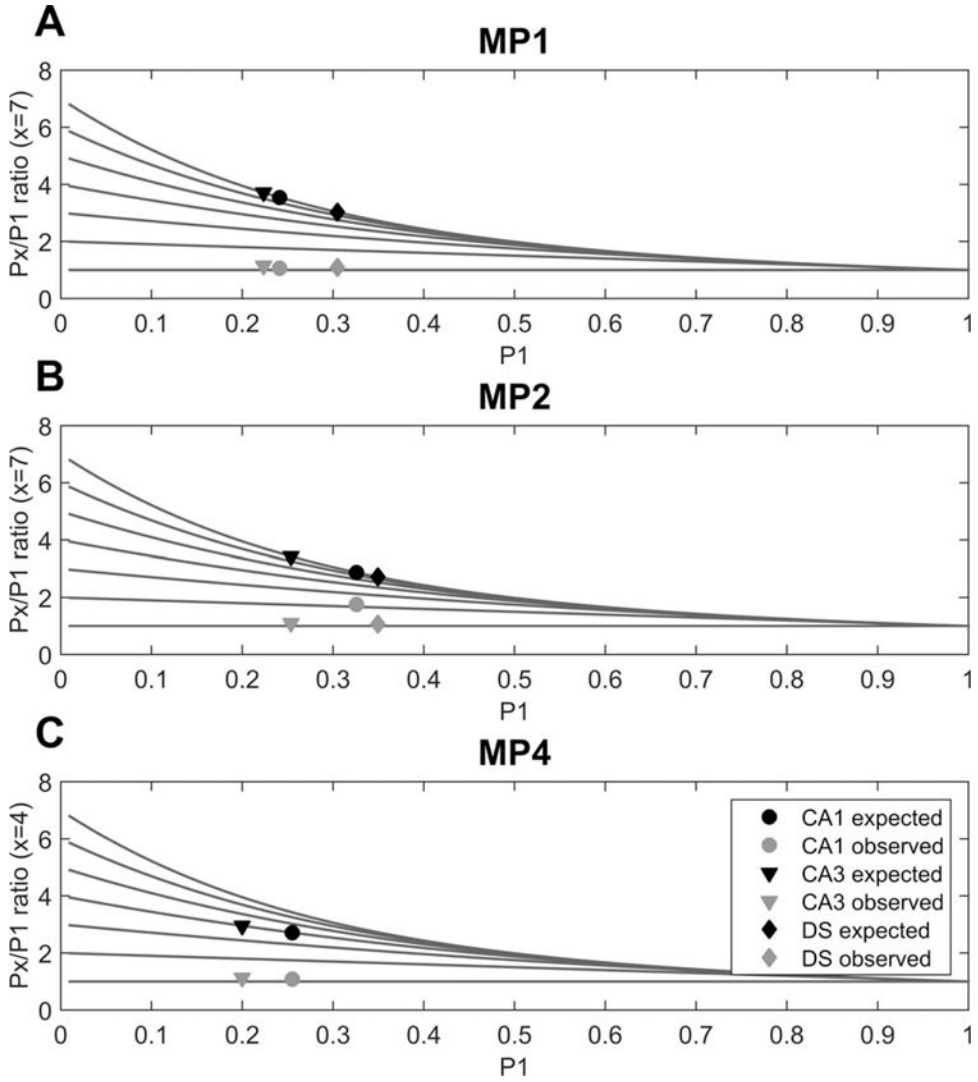

FIGURE 1.

Representative results from three IEG studies illustrating the observed activation ratios (P_x/P_1) and the ratios expected on the basis of URDWR. The expected recruitment proportions (black symbols) are predicted ratios derived from the URDWR model. In all studies shown, URDWR predictions overestimate the actual activation proportions (grey symbols). A) Representative ratios of expected versus observed activation ratios in CA1, CA3, and dorsal subiculum in study MP1 and B) study MP2. This overestimation is consistent across CA1, CA3 and dorsal subiculum (DS). Note also that there is a systematic difference in the P_1 values across subregions, consistent with observations from recording studies. C) Study MP4 shows activation data from CA1 and CA3 from the same tissue as the original study on dentate gyrus published by Alme *et al.*, (2010). Note that in all experiments and hippocampal subregions, the observed activation ratios fall substantially short of the ratios expected on the basis of URDWR.

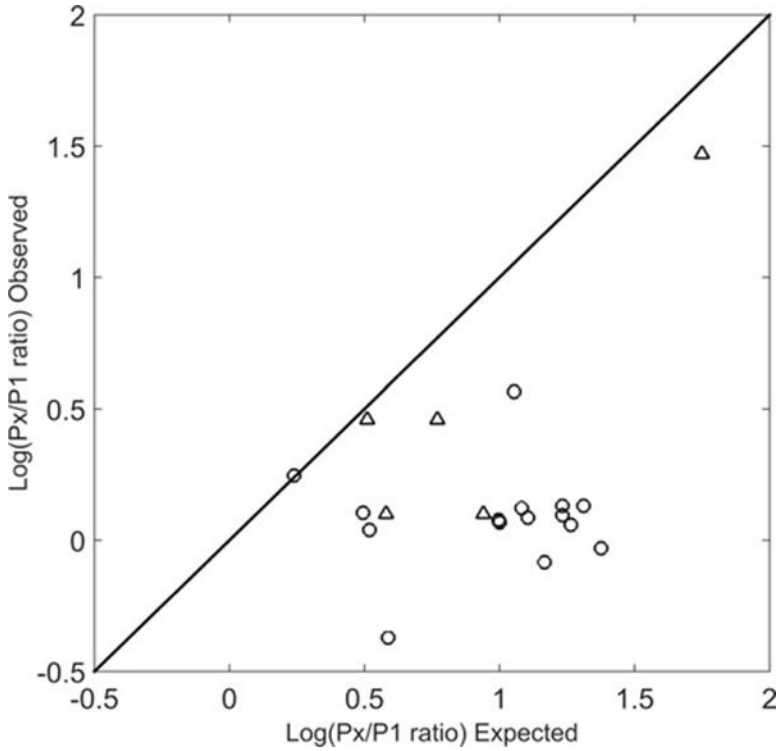

FIGURE 2.

Summary of activation ratios, plotted on a log-log scale (values reported in Table 1 in parentheses), from seven IEG studies (o symbol) and two unit recording studies (Δ symbol) for which data were available showing the overall relationship between expected activation ratio under URDWR and observed activation ratio. The expected ratio approaches 1 in the case of either a small relative difference in environment sizes or a large value of P_1, which is itself expected to approach 1.0 as the initial environment size for which P_1 is estimated increases The solid line represents agreement between observed and expected. Note that although the expected ratio of counts from larger and smaller environments is always greater than 1.0 under URDWR, due to random variation and/or sampling error, in some experiments the counts for the larger environments actually fell slightly below those for the smaller environment, resulting in observed ratios less than one. The general pattern of results across the majority of experiments is that the observed ratios fall far short of the URDWR expectation. Note also that the number of data points exceeds the number of studies due to sampling of multiple hippocampal subfields.

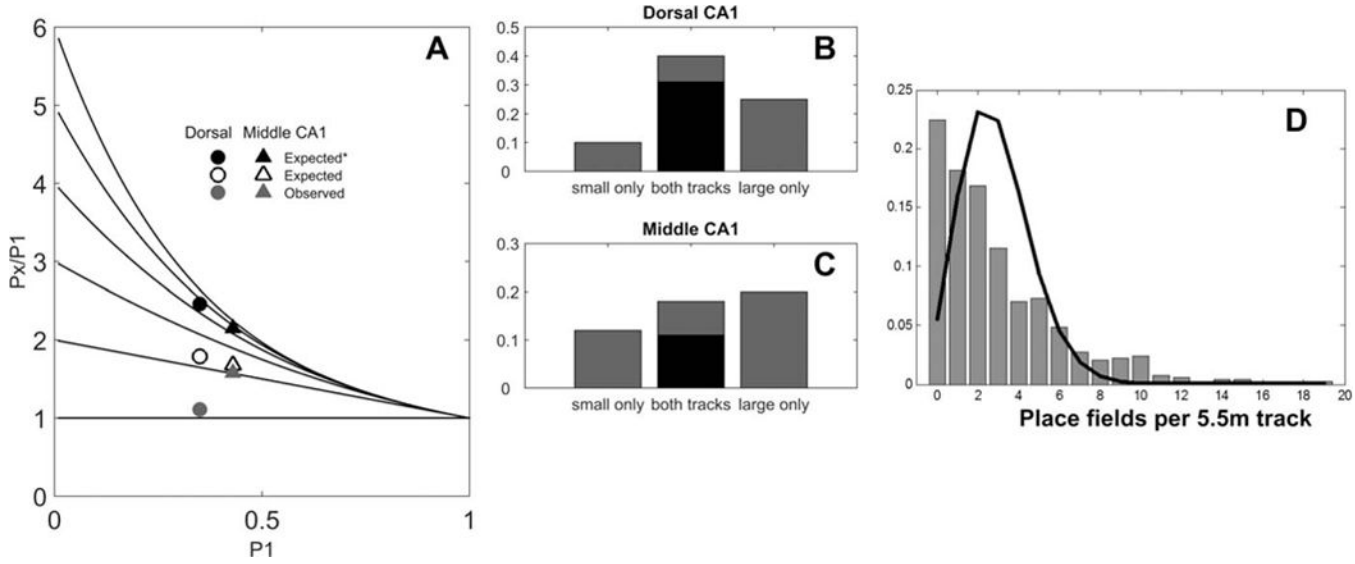

FIGURE 3.

A) Comparison of observed activation ratios on both the small and large tracks in the Maurer *et al.* (2006) recording study versus the expected ratios assuming URDWR. Considering the ratios of track circumference as 4.6:1* or 2.3:1, in either case the actual measures of activation fall below the URDWR expectation. B) Proportion of dorsal CA1 cells exhibiting place fields on either the small track only, large track only, or both are shown in grey. Expected overlap is shown in black. C) Proportion of middle CA1 cells exhibiting place fields on either the small track only, large track only, or both are shown in grey. Expected overlap is shown in black. D) Number of place fields expressed by dorsal CA1 neurons in the study by Maurer *et al.* (2006), compared to the Poisson prediction for the same mean. Note that the actual data included substantially more cells with no fields than the Poisson prediction. For illustration, we pooled the place field counts for the large and small tracks (total length 5.5 m) for all of the recorded dorsal hippocampal neurons and computed the Poisson prediction from the mean number of fields.

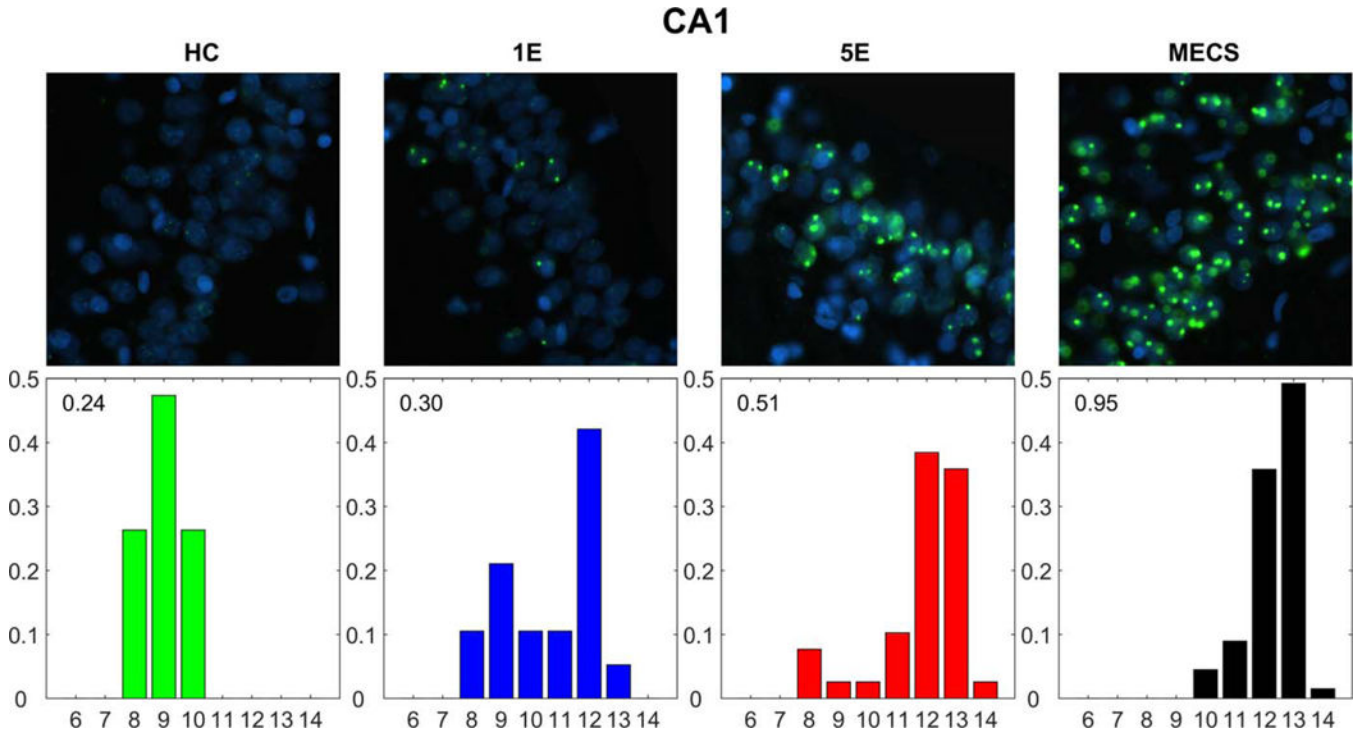

FIGURE 4.

Representative wide field fluorescence images of CA1 nuclei expressing *H1a* intranuclear transcription foci (INF) from study MP2 illustrating the range of INF size and brightness (HC = home cage control; 1E = one environment; 5E = five environments, MECS = positive control). Beneath each image is the corresponding histogram of log-integrated intensities of Homer1a INFs depicted (normalized counts; numbers in corner reflect proportion of positive nuclei). In this experiment, a very low detection criterion was set in order to capture nearly the full range of INF size and intensity. INFs were counted and an integrated intensity score was calculated for each segmented INF by summing the green channel pixel intensity. Note that with this procedure the integrated intensity score will not necessarily exhibit a sharp lower bound because of the dual criteria for passing threshold in the INF identification process. It should be noted, however, that the automated counting results correlated highly with manual counts by several experienced counters. [Color figure can be viewed in the online issue, which is available at wileyonlinelibrary.com.]

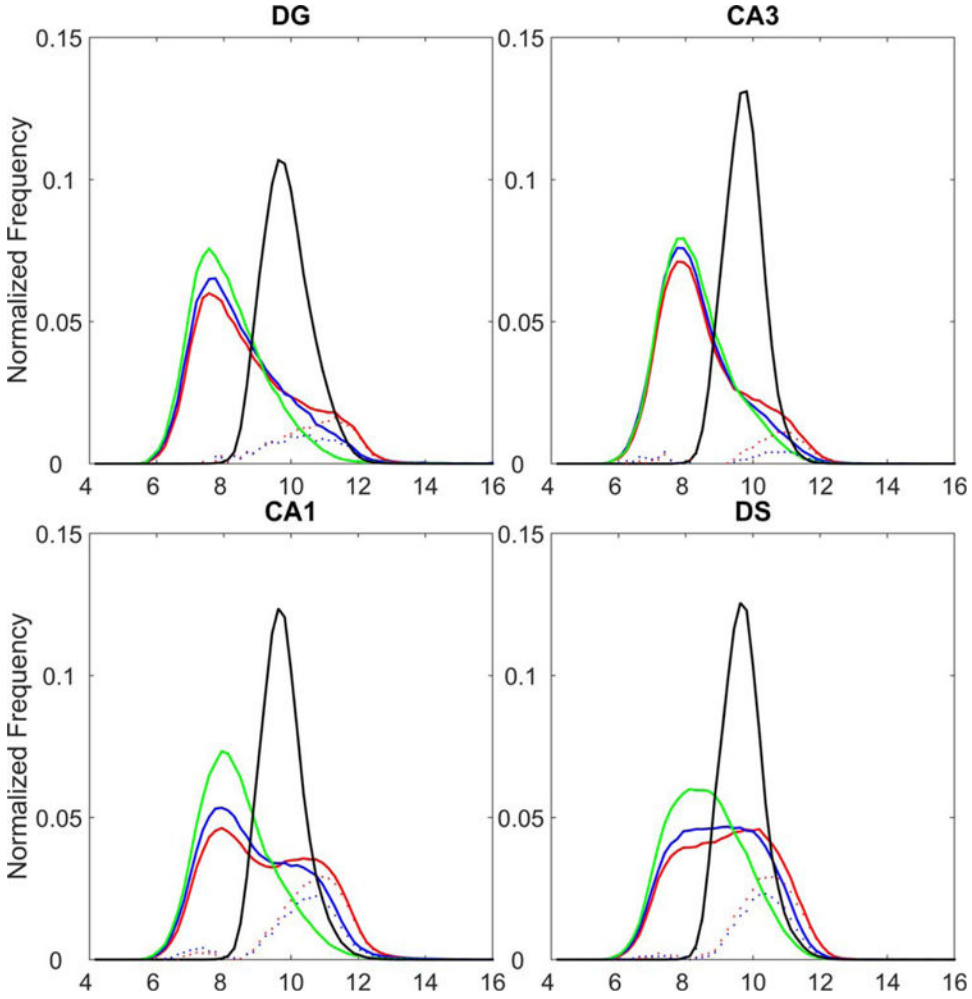

FIGURE 5.

Relative frequency distributions for *H1a* INF log integrated intensities (integral of pixel intensity over the segmented INF) from study MP2 (green = caged control; blue = 1E; red = 5E; black = MECS). Histograms for each condition and hippocampal subfield are normalized to their respective total counts (i.e., sum to 1.0). Actual relative count data (proportion of *H1a* positive nuclei relative to MECS) are given in Figure 6. Number of *H1a* INF (pooled across subjects) contributing to each histogram are: HC 194,308; 1E 351,197; 5E 440,738; MECS 153,676. The distributions of INF intensity during rest in home cage is highly positively skewed, appearing almost unimodal log-normal (green traces). Exposure to one environment (blue) leads to increased skew or bimodality in the log plot due to the increased activation of a fraction of neurons. Exposure to five environments (red) increases the intensity of some INFs but does not substantially increase the number of detected (above threshold) INFs (see Fig. 6). Exposure to maximal electroconvulsive shock (black), which activates most IEG competent neurons, produces a unimodal high integrated intensity log-normal distribution, and many more counts (Fig. 6). Note that the INF segmentation algorithm involves a threshold which causes some underestimation of the numbers of very small, dim INFs and hence may underestimate the left tails of the distributions. It is clear from these histograms and the counts shown in Figure 6, that, rather

than adding a significant number of INF counts, the exposure to one and five environments shifted some of the INFs from the home cage distribution to a higher volume and intensity distribution that overlaps the home cage distribution. The dashed red and green curves represent the residuals after fitting the home cage distributions to the data and subtracting. See text for further description. [Color figure can be viewed in the online issue, which is available at wileyonlinelibrary.com.]

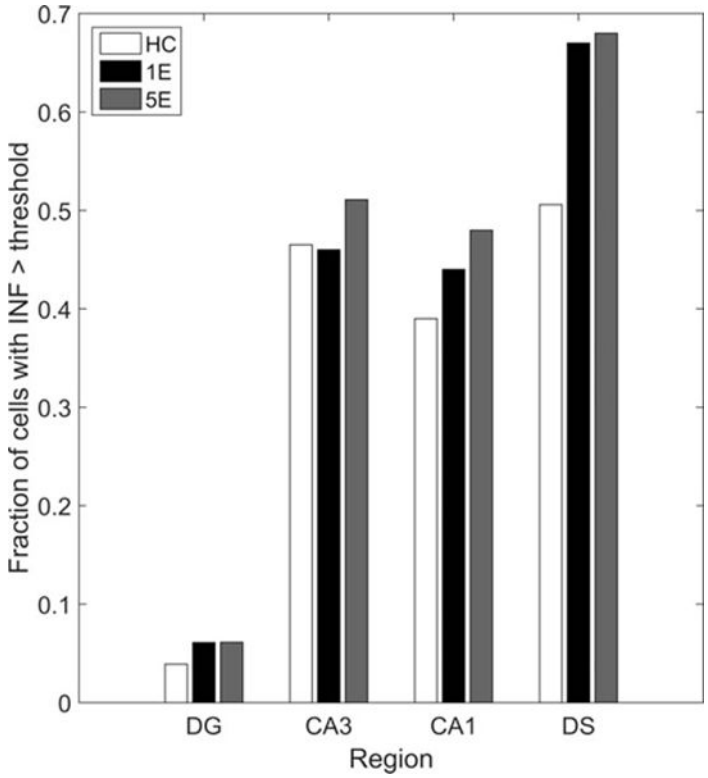

FIGURE 6.

Homer1a INF counts from Experiment MP2 for home cage (HC) one environment (1E) and 5 environment (5E) conditions. For this analysis, the total number of nuclei in the regions of interest was estimated by taking the sum over all blue (DAPI) pixels in the ROI and dividing by the average sum for a sample of manually segmented nuclei from the same region, without correction for glia. The proportion of these nuclei that were IEG competent neurons was estimated from a separate set of animals exposed to maximal electroconvulsive shock (MECS), which induces expression in all competent neurons. These proportions differed across regions [DG = 0.90; CA3 = 0.55; CA1 = 0.64; DS = 0.52] due to the varying number of glia and non IEG expressing neurons in the different fields. The fraction of neurons expressing above threshold INFs in the three experimental conditions was adjusted by the corresponding regional MECS INF + fractions. In all four hippocampal subfields, the number of counts in the 1E and 5E conditions do not differ significantly. Note, however, that the counts include both the low and high intensity INFs visible in the bimodal distributions in Figure 5. Thus, for example, although the 1 and 5 environment counts are hardly above the home cage counts, this does not take into account that in the latter conditions there was a more substantial relative increase in high intensity INFs and decrease in low intensity INFs.

TABLE 1

Observed Versus URDWR-Predicted Activation Measures from Seven IEG and Two Electrophysiological Experiments, as Represented in Figure 2

Study	*x (ratio of areas in multi vs. single env. groups)*	Region	P_1	P_x	Assuming URDWR: Expected P_x/P_1 (log)	Observed P_x/P_1 (log)
IEG Experiments						
MP1	7	CA1	0.2411	0.2555	3.54 (1.26)	1.06 (0.06)
	7	CA3	0.2234	0.2549	3.71 (1.31)	1.14 (0.13)
	7	DS	0.3048	0.3310	3.02 (1.11)	1.09 (0.09)
MP2	7	CA1	0.3260 *	0.5750 *	2.87 (1.05)	1.76 (0.56)
	7	CA3	0.2537	0.2811	3.43 (1.23)	1.10 (0.10)
	7	DS	0.3495	0.3561	2.72 (1.00)	1.07 (0.07)
MP3	5	CA1	0.2240	0.2060	3.21(1.17)	0.92 (−0.08)
	5	CA3	0.1170	0.1130	3.96 (1.38)	0.97 (−0.03)
MP4	4	CA1	0.2550	0.2750	2.71 (1.00)	1.08 (0.08)
	4	CA3	0.2000	0.2250	2.95 (1.08)	1.13 (0.12)
CT5	4	CA1	0.2318	0.2644	3.43 (1.23)	1.14 (0.13)
AB6	2	CA1	0.7300	0.5700	1.27 (0.24)	1.28 (0.25)
	2	CA3	0.3600	0.4000	1.64 (0.49)	1.11 (0.10)
AB7	2	CA1	0.3200	0.3300	1.68 (0.52)	1.04 (0.04)
	2	CA3	0.2000	0.1400	1.80 (0.59)	0.69 (−0.37)
Electrophysiology Experiments						
Maurer et al., 2006	2.3	Dorsal CA1	0.43	0.68	1.68 (0.51)	1.58 (0.46)
		middle CA1	0.35	0.39	1.79 (0.58)	1.11 (0.10)
	4.6	Dorsal CA1	0.43	0.68	2.15 (0.77)	1.58 (0.46)
		Middle CA1	0.35	0.39	2.46 (0.94)	1.11 (0.10)
Alme et al., 2014	11	CA3	0.14	0.61	5.78 (1.75)	4.35 (1.47)

For each study, the corresponding increase in area sampled in the multiple-environment test group is expressed as “x ratio of areas” when activation in the multiple-environment test groups was compared to the single-environment test group. P_1 and P_X denote the average activation proportions in each subregion observed in the single-environment group and multiple-environment group, respectively, by counting cells that exhibited IEG expression or clear place fields. Expected P_X/P_1 is the hypothetical ratio of activation proportions assuming URDWR is true.

* Probabilities (P_1 and P_X) used for calculations have been home-cage subtracted if home-cage activation was available.

TABLE 2

Activation of Neurons in Different Hippocampal Subfields After Exposure to One and Five Environments in Experiments MP1 and MP2

Study MP1	DG	CA3	CA1	DS
P_1	0.037	0.094	0.246	0.197
Observed ratio	1.099	1.473	1.268	1.408
Expected ratio	4.645	4.143	3.075	3.383

Study MP2	DG	CA3	CA1	DS
P_1	0.009	0.020	0.119	0.161
Observed ratio	1.477	2.663	1.480	1.440
Expected ratio	4.914	4.800	3.944	3.627

P_1 represents the total proportion of activated neurons based on the INF integrated intensity analysis outlined in Figures 5 and 6, and described in the text. Observed ratio is the ratio of activation for five environments vs one environment, whereas Expected ratio refers to the URDWR prediction. Although the actual area ratios were about 7.2:1, we have used 5:1 as a more conservative estimate here (in contrast to 7:1 as previously shown in Table 1 and Fig. 2), based on the fact that exposure times were equal in all environments and the animals likely did not visit the entire environments in the available time. In all cases, the observed ratio is substantially less than the expected ratio.